Available online at www.sciencedirect.com
ScienceDirect
Journal of Hazardous Materials 143 (2007) 690–701
Journal of Hazardous Materials
www.elsevier.com/locate/jhazmat

Finite element modeling of contaminant transport in soils including the effect of chemical reactions

A.A. Javadi *, M.M. AL-Najjar

Department of Engineering, University of Exeter, Exeter, Devon EX4 4QF, UK

Available online 9 January 2007

Abstract

The movement of chemicals through soils to the groundwater is a major cause of degradation of water resources. In many cases, serious human and stock health implications are associated with this form of pollution. Recent studies have shown that the current models and methods are not able to adequately describe the leaching of nutrients through soils, often underestimating the risk of groundwater contamination by surface-applied chemicals, and overestimating the concentration of resident solutes. Furthermore, the effect of chemical reactions on the fate and transport of contaminants is not included in many of the existing numerical models for contaminant transport. In this paper a numerical model is presented for simulation of the flow of water and air and contaminant transport through unsaturated soils with the main focus being on the effects of chemical reactions. The governing equations of miscible contaminant transport including advection, dispersion–diffusion and adsorption effects together with the effect of chemical reactions are presented. The mathematical framework and the numerical implementation of the model are described in detail. The model is validated by application to a number of test cases from the literature and is then applied to the simulation of a physical model test involving transport of contaminants in a block of soil with particular reference to the effects of chemical reactions. Comparison of the results of the numerical model with the experimental results shows that the model is capable of predicting the effects of chemical reactions with very high accuracy. The importance of consideration of the effects of chemical reactions is highlighted.

Keywords: Contaminant transport; Unsaturated soil; Finite element; Chemical reaction

1. Introduction

In recent years, interest in understanding the mechanisms and prediction of contaminant transport through soils has dramatically increased because of growing evidence and public concern that the quality of the subsurface environment is being adversely affected by industrial, municipal and agricultural activities. Transport phenomena are encountered in almost every aspect of environmental engineering science. In assessing the environmental impacts of waste discharges it is important to predicate the impact of emission on contaminant concentration in nearby air and water [25]. Contamination of groundwater is an issue of major concern in residential areas which may occur as a result of spillages of hazardous chemicals, dumping of toxic waste, landfills, waste water, or industrial discharges [9]. Hazardous waste disposal is increasingly becoming one of the most serious problems confronting health and the environment. The movement of chemicals through the soil to the groundwater represents a degradation of these resources. In many cases, serious human and stock health implications are associated with this form of pollution. One of the most challenging problems in modeling of solute transport in soils is how to effectively characterize and quantify the geometric, hydraulic, and chemical properties of porous media. During the past two decades, attempts have been made to develop physical, analytical and numerical models for contaminant transport through soils considering the effects of different transport mechanisms. Abriola and Pinder [1] developed a general model that addressed the multiphase flow problem and the transport of organic species. Celia and Bololoutas [6] presented a numerical technique for the solution of advection–diffusion type of transport equation. Li et al. [19] developed a numerical model to simulate contaminant transport through soils taking into account the influence of mechanisms of the miscible contaminant transport including advection, mechanical dispersion, molecular diffusion and adsorption. Karkuri and Molenkamp [17] presented a formulation for groundwater flow and pollutant transport through multi-layered saturated soils in one

* Corresponding author. Tel.: +44 1392 263640; fax: +44 1392 217965.
E-mail addresses: a.a.javadi@ex.ac.uk (A.A. Javadi), m.m.al-najjar@ex.ac.uk (M.M. AL-Najjar).

0304-3894/$ – see front matter © 2007 Elsevier B.V. All rights reserved.
doi:10.1016/j.jhazmat.2007.01.016

dimension. Sheng and Smith [31] used a finite element method for the solution of the advection–dispersion transport equation for multicomponent contaminations. Zhang and Brusseau [45] developed a mathematical model incorporating the primary mass transfer processes that mediate the transport of immiscible organic liquid constituents in water-saturated, locally heterogeneous porous media. Yan and Vairavmoorthy [42] developed a numerical model to simulate water flow and contaminant transport through homogeneous partially saturated media by using the finite difference technique. Kacur et al. [16] presented a numerical approximation scheme for the solution of contaminant transport with diffusion and adsorption by finite volume method.

Inclusion of chemical effects in solute transport simulation has continued to evolve although numerous difficulties still limit development in this field. Rubin and James [29] provided an early example of a mathematical transport model with equilibrium-controlled reactions. Rubin [28] described the mathematical requirements for simulation of several classes of reaction, and noted the computational difficulties presented by various systems. Extensive research has been carried out on the biodegradation of organic chemicals in the subsurface, leading to methods of approximating some biodegradation effects in transport calculations. Parkhurst et al. [27] provided a mathematical basis for the incorporation of inorganic equilibrium reactions in solute transport analysis. A summary of chemical processes in groundwater is provided by Gillham and Cherry [12] and Cherry et al. [7]. Ahuja and Lehman [2] and Snyder and Woolhiser [32] presented experimental results that indicated that a more detailed description of chemical transport in soil and water was needed. A review of coupling transport simulation with both equilibrium-controlled and kinetic reactions is provided by Yeh and Tripathi [43]. In spite of numerous mathematical models that have been developed to simulate the migration of pollutants in soils, still, majority of the existing models concentrate on either geochemical processes [10,41] or biological transformations [18,8]. Only a limited number of models include chemical reactions in soils. Mironenko and Pachepsky [24] simulated the accumulation of a chemical transported from soil to ponding water. They considered one-dimensional convective-diffusive solute transport in water and soil. Their results showed that the relative effect of diffusion on the accumulation of a solute in ponding water may be significant at infiltration rates that are not uncommon in agriculture practice. Wallach et al. [40] introduced a mathematical model for transport of soil dissolved chemicals by overland flow. The model can predict water flow and chemical transport in the soil profile prior to the rainfall ponding and during the surface runoff event. The model was used to investigate the dependence of surface runoff pollution and its extent on the system hydrological parameters. Arsene [4] presented the migration assessment of (^{3}H ^{14}C and ^{241}AM) in unsaturated soil as the emplacement medium for the disposal of conditioned wastes. Gao et al. [11] presented a model for simulating the transport of chemically reactive components in groundwater systems. McGrail [23] developed a numerical simulator to assist in the interpretation of complex laboratory experiments examining transport processes of chemical and biological contaminants subject to nonlinear adsorption or source terms. The governing equations for the problem were solved by the method of finite differences. The sources for surplus of soil nitrogen, such are fertilization farm waste disposal and improper agro-technical management, were studied in controlled field experiments [37] and in real life farming practice [36]. More recently, Stoicheva et al. [38] reported results from an experimental investigation into the nitrogen distribution in geological materials underlying soils under natural and anthropogenic loading in different agro-climatic regions in Bulgaria. Osinubi and Nwaiwu [26] evaluated the nature of sodium diffusion in compacted soils through laboratory adsorption and diffusion tests on three lateritic soils. Recent studies have shown that current models and methods do not adequately describe the leaching of nutrients through soil, often underestimating the risk of groundwater contamination by surface-applied chemicals, and overestimating the concentration of resident solutes [33]. This information is vital in evaluation of existing theoretical models and development of improved conceptual models of transport processes. The high costs, large time scales and lack of control over the boundary conditions have prevented the development of field scale experiments [13]. Stagnitti et al. [33] investigated the effects of chemical reactions on contaminant transport through a number of physical model tests on an undisturbed block of soil. Despite the development of conceptual and mathematical models for the effects of chemical reactions on contaminant transport, majority of the existing numerical models do not include the effect of chemical reactions on the concentration and transport of contaminants in soil. Therefore, the focus of this paper is the development, validation and application of a coupled transient finite element model for contaminant transport in unsaturated soils that incorporates the effects of chemical reactions on the contaminant transport. In what follows, the main governing phenomena of miscible contaminant transport including advection, mechanical dispersion, molecular diffusion and adsorption are considered together with the effect of the chemical reactions. The contaminant transport equation and the balance equations for flow of water and air are solved numerically using the finite element method, subject to prescribed initial and boundary conditions. The developed model is validated by comparing the model prediction results with those reported in the literature. The model is also applied to a case study involving measurements of the effects of chemical reactions on the solute transport process. It is shown that the developed model is capable of predicting, with a good accuracy, the variations of the contaminant concentration with time considering the effect of chemical reactions.

2. Governing equations of fluid flow and contaminant transport in soil

The introduction outlined a broad range of issues that are of interest in relation to transport of contaminant in soils. The problem becomes more complex when the soil is unsaturated. Unsaturated soil is a multiphase system, because at least two fluid phases are present: water and air. The governing equations that describe fluid flow and contaminant transport in the unsaturated zone will be presented in this section.

2.1. Modeling of water flow

The governing differential equation for water flow is based on the conservation of mass of the ground water, leading to [39]:

$$c_{ww}\left(\frac{\partial u_w}{\partial t}\right) + c_{wa}\left(\frac{\partial u_a}{\partial t}\right) = \nabla(K_{ww}\nabla u_w) + \nabla(K_{wa}\nabla u_a) + J_w \quad (1)$$

where $c_{ww} = c_{fw} + c_{vw}$; $c_{wa} = c_{fa} + c_{va}$; $c_{vw} = nS_aK_{fw}$; $c_{va} = nS_aK_{fa}$; $c_{fw} = -n(\rho_w - \rho_v)\partial S_w/\partial s$; $c_{fa} = n(\rho_w - \rho_v)\partial S_w/\partial s$; $K_{ww} = \rho_w K_w/\gamma_w + K_{vw}\rho_w$; $K_{wa} = \rho_v K_a + \rho_w K_{va}$; $K_{fa} = \rho_0 \partial h/\partial\psi\partial\psi/\partial s\nabla u_a$; $K_{fw} = -\rho_0\partial h/\partial\psi\partial\psi/\partial s\nabla u_w$; $K_{vw} = -(D_{atms}V_v n/\rho_w)k_{fw}$; $K_{va} = -(D_{atms}V_v n/\rho_w)K_{fa}$; $J_w = \rho_w\nabla(K_w\nabla z)$ in which n is the porosity of the soil, K_w the conductivity of water $[L][T]^{-1}$, K_a the conductivity of air $[L][T]^{-1}$, S_w the degree of saturation of water, S_a the degree of saturation of air, ρ_w the density of water $[M][L]^{-3}$, ρ_v the density of water vapor $[M][L]^{-3}$, ρ_0 the density of saturated soil vapor $[M][L]^{-3}$, s the soil suction $[M][L]^{-1}[T]^{-2}$, V_v the mass flow factor, u_w the pore-water pressure $[M][L]^{-1}[T]^{-2}$, u_a the pore-air pressure $[M][L]^{-1}[T]^{-2}$, D_{atms} the molecular diffusivity of vapor through air, γ_w the unit weight of water $[M][L]^{-2}[T]^{-2}$, ψ the capillary potential, h the relative humidity and ∇z is the unit normal oriented downwards in the direction of the force of gravity.

2.2. Modeling of air flow

The governing differential equation for air flow is based on the conservation of mass of the ground air, leading to [39]:

$$c_{aw}\left(\frac{\partial u_w}{\partial t}\right) + c_{aa}\left(\frac{\partial u_a}{\partial t}\right) = \nabla(K_{aw}\nabla u_w) + \nabla(K_{aa}\nabla u_a) + J_a \quad (2)$$

where $c_{aw} = c_{aw1} + c_{aw2}$; $c_{aa} = c_{aa1} + c_{aa2}$; $c_{aw1} = -n\rho_{da}(H_a - 1)\partial S_w/\partial s$; $c_{aa1} = n\rho_{da}(H_a - 1)\partial S_w/\partial s$; $c_{aw2} = n(S_a + H_aS_w)c_{daw}$; $c_{aa2} = n(S_a + H_aS_w)c_{daa}$; $c_{daw} = -(R_v/R_{da})K_{fw}$; $c_{daa} = 1/R_{da}T - (R_v/R_{da})K_{fa}$; $K_{aw} = (H_a\rho_{da}/\gamma_w)K_w$; $K_{aa} = K_a\nabla u_w$; $J_a = H_a\rho_{da}\nabla(K_w\nabla z)$ in which H_a is the Henry's volumetric coefficient of solubility, ρ_{da} the density of dry air $[M][L]^{-3}$, R_{da} the specific gas constant for dry air and R_v is the specific gas constant for water vapor.

2.2.1. Advection

Advection is the transport of material caused by the net flow of the fluid in which that material is suspended. Whenever a fluid is in motion, all contaminants in the flowing fluid, including both molecules and particles, are advected along with the fluid [25]. The rate of contaminant transport that occurs by advection is given by the product of contaminant concentration c and the component of apparent groundwater velocity like v_x, v_y, etc. For two-dimensional cases with two components of the contaminant transport in the x and y directions, the rate of contaminant transport due to advection will be [14]:

$$F_{x,\text{advection}} = v_{wx}c \quad (3a)$$

$$F_{y,\text{advection}} = v_{wy}c. \quad (3b)$$

2.2.2. Diffusion

The process by which contaminants are transported by the random thermal motion of contaminant molecules is called diffusion [44]. The rate of contaminant transport that occurs by diffusion is given by Fick's law. In terms of two component of the contaminant transported in the x and y directions, the rate of contaminant transport by diffusion will be [14]:

$$F_{x,\text{diffusion}} = -D_m\frac{\partial c}{\partial x} \quad (4a)$$

$$F_{y,\text{diffusion}} = -D_m\frac{\partial c}{\partial y} \quad (4b)$$

where D_m is the molecular diffusion coefficient in the porous medium $[L]^2[T]^{-1}$.

2.2.3. Mechanical dispersion

Mechanical dispersion is a mixing or spreading process caused by small-scale fluctuation in groundwater velocity along the tortuous flow paths within individual pores. In terms of two component of contaminant transport in x and y directions, the rate of contaminant transport by mechanical dispersion is given by

$$F_{x,\text{dispersion}} = -D_{wxx}\frac{\partial}{\partial x(\theta_w c)} - D_{wxy}\frac{\partial}{\partial y(\theta_w c)} \quad (5a)$$

$$F_{y,\text{dispersion}} = -D_{wyx}\frac{\partial}{\partial x(\theta_w c)} - D_{wyy}\frac{\partial}{\partial y(\theta_w c)} \quad (5b)$$

where D_{wxx}, D_{wxy}, D_{wyx}, D_{wyy} are the coefficients of dispersivity tensor $[L][T]^{-1}$. For water phase these coefficients can be computed from the following expressions [30]:

$$D_{wxx} = \alpha_{TW}|v_w|\delta_{xx} + \frac{(\alpha_{LW} - \alpha_{TW})\bar{v}_{w_x}\bar{v}_{w_x}}{|v|} + D_{m_w}\delta_{xx} \quad (6a)$$

$$D_{wyy} = \alpha_{TW}|v_w|\delta_{yy} + \frac{(\alpha_{LW} - \alpha_{TW})\bar{v}_{w_y}\bar{v}_{w_y}}{|v|} + D_{m_w}\delta_{yy} \quad (6b)$$

$$D_{wxy} = D_{wyx} = \frac{(\alpha_{LW} - \alpha_{TW})\bar{v}_{w_x}\bar{v}_{w_y}}{|v|} + D_{m_w}\delta_{xy} \quad (6c)$$

where α_{TW} is the transverse dispersivity (L) for water phase, α_{LW} the longitudinal dispersivity (L) for water phase, δ_{ij} the Kroneker delta ($\delta_{ij} = 1$ when $i = j$, $\delta_{ij} = 0$ otherwise), $|v|$ the magnitude of the water velocity ($|v| = \sqrt{\bar{v}_{w_x}^2 + \bar{v}_{w_y}^2}$), θ_w the volumetric water content, D_{m_w} the coefficient of water molecular diffusion $[L]^2[T]$ and $\bar{v}_{w_x}$ and $\bar{v}_{w_y}$ are the components of the water velocity computed as $\bar{v}_{w_x} = v_x/\theta_w$ and $\bar{v}_{w_y} = v_y/\theta_w$. The amount of contaminant in each phase (α) is denoted by the mass fraction, which is defined as

$$\omega_\alpha = \frac{\text{mass of contaminant in phase }(\alpha)}{\text{mass of phase }(\alpha)} \quad (7)$$

The standard mass balance equation of contaminant transport can then be written as [15]

$$\frac{\partial(\theta_w \rho_w \omega_w)}{\partial t} + F_{\text{advection}} - F_{\text{dispersion–diffusion}} + \lambda_w \theta_w \rho_w \omega_w = F^w \quad (8)$$

where λ_w is the reaction rate for water $[T]^{-1}$ and F^w is the source/sink term for water $[M][L]^{-3}[T]^{-1}$. In the transport Eq. (8), the first term describes the change of contaminant mass in time; the second represents the movement of contaminant due to advection and the third term represents the effects of dispersion (which is assumed to be Fickian in form with the dispersion tensor given by Bear [5]. In the forth term the contaminants are assumed to be reactive with a decay rate of (λ), and the right hand side term describes sources and sinks in the equation. Rather than using the contaminant mass fraction it is often more convenient to use the volumetric concentration (c_α) which is defined as

$$c_\alpha = \frac{\text{mass of contaminant in phase } (\alpha)}{\text{volume of phase } (\alpha)} = \rho_\alpha \omega_\alpha \quad (9)$$

In most of the work presented in this paper, the contaminant volumetric concentration in water will be used. The governing equation can be rewritten in terms of c by substituting the above relation into the governing equation:

$$\frac{\partial(\theta_w c_w)}{\partial t} + \left(\frac{\partial}{\partial x(v_{wx} c)} + \frac{\partial}{\partial y(v_{wy} c)}\right) - \left(\frac{\partial}{\partial x}\left(D_{wxx}\frac{\partial c}{\partial x} + D_{wxy}\frac{\partial c}{\partial y}\right) + \frac{\partial}{\partial x}\left(D_{wyy}\frac{\partial c}{\partial y} + D_{wyx}\frac{\partial c}{\partial x}\right)\right)\theta_w + \lambda_w \theta_w c_w = F^w \quad (10)$$

In the numerical model presented in this work sorption of the contaminant onto the solid phase, in addition to advection, diffusion and dispersion, is considered.

2.2.4. Adsorption

When a porous medium is saturated with water containing dissolved matter, it frequently happens that certain solutes, to 1° or another, are removed from solution and immobilized in or on the solid matrix of the porous medium by electrostatic or chemical forces. Adsorption refers to adherence of chemical species primarily on the surface of the porous matrix. The main factors affecting the adsorption of pollutants to or from the solid are the physical and chemical characteristics of the considered pollutant and of the surface of the solid [19]. The amount of sorption is generally dependent on the contaminant and the composition of the soil. Using the assumption that adsorption only occurs from the water to the solid phase, the equation for the water phase can be modified to include adsorption [15]:

$$\frac{\partial(\theta_w c_w)}{\partial t} + \frac{\partial}{\partial t(\theta_s \rho_s K_d c_w)} + \nabla(v_w c_w) - \nabla(\theta_w D_w \nabla c_w) + \lambda_w \theta_w c_w = F^w \quad (11)$$

where K_d is the distribution coefficient. In the case of sorption the equation for the water phase is modified to include a retardation factor. The principal assumption used in deriving a retardation factor is that water is the wetting fluid so that the air phase does not have any contact with the solid phase [46]. Therefore, the equation can be rewritten as

$$\frac{\partial(R\theta_w c_w)}{\partial t} + \nabla(v_w c_w) - \nabla(\theta_w D_w \nabla c_w) + \lambda_w \theta_w c_w = F^w \quad (12)$$

where R is the retardation coefficient $= [1 + \theta_s \rho_s K_d/\theta_w]$, ρ_s is the density of the solid phase and θ_s is the volumetric content of the solid phase.

The transport of contaminant in the soil by external and internal effects will result in reactions occurring between contaminant and soil constituents. These include chemical, physical and biological processes [44]. Most chemical reactions affecting solute transport can be divided broadly into two groups [46]:

1. Those that are "sufficiently fast" and reversible, so that local equilibrium can be assumed (i.e., reactions that can be assumed to reach equilibrium in each locality within the residence times characterizing the transport regime).
2. Those that are "insufficiently fast" and irreversible, so that the local equilibrium assumption is not appropriate.

Under each group, Rubin [28] made a further distinction between "homogeneous" reactions that take place within a single phase, and "heterogeneous" reactions that involve more than one phase. The heterogeneous classes of reactions are the surface reactions (i.e., sorption and ion exchange) and classical reactions (i.e., precipitation/dissolution, oxidation/reduction or redox and complexation). This classification scheme leads to six classes of reactions as illustrated in Fig. 1. The effects of chemical reactions on solute transport are generally incorporated in the advection, diffusion–dispersion and adsorption equations through additional terms [46]. Consider a chemical reaction as

$$aA + bB \rightleftarrows rR + sS \quad (13)$$

where a, b, r and s are the valences for ions. A general kinetic rate law for species A can be expressed as [46]

$$\frac{\partial c_A}{\partial t} = -\lambda c_A^{n1} c_B^{n2} + \gamma c_R^{m1} c_S^{m2} \quad (14)$$

where c_A, c_B, c_R and c_S are concentrations of reactant species A and B and resultant species R and S, respectively; λ and γ are the rate constants for the forward and reverse reactions, respectively; $n1$, $n2$ and $m1$, $m2$ are empirical coefficients. The sum of $n1$ and $n2$ defines the order of the forward reaction while the sum of $m1$ and $m2$ defines the order of the reverse reaction. Eq. (14) expresses the rate of change in species A as the sum of the rates at which it is being used in the forward reaction and generated in the reverse reaction. Certain chemical reactions such as radioactive decay, hydrolysis and some forms of biodegradation can be characterized as first order, irreversible processes [46].

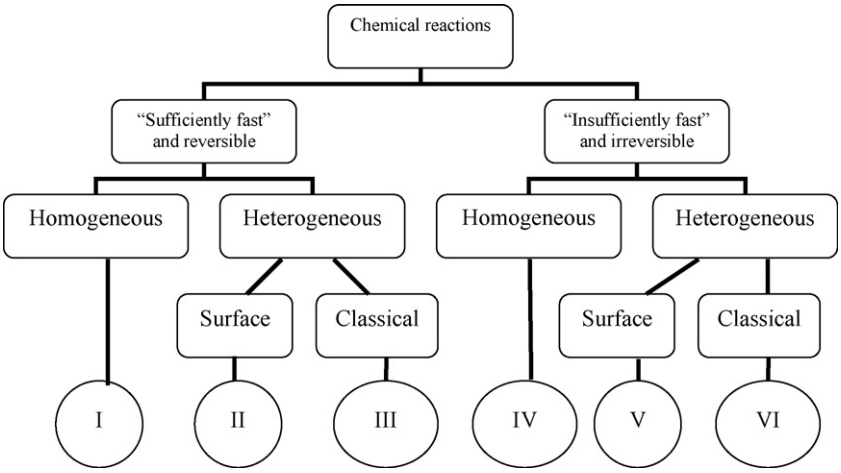

Fig. 1. Classification of chemical reactions useful in solute transport analyses [46].

In this type of reaction Eq. (14) simplifies to:

$$\frac{\partial c}{\partial t} = -\lambda c. \tag{15}$$

Chemical reactions can be classified into four general types [20]:

1. *Synthesis reaction*: In a synthesis reaction two or more simple substances combine to form a more complex substance. Two or more reactants yielding one product are another way to identify a synthesis reaction.
2. *Decomposition reaction*: In a decomposition reaction a more complex substance breaks down into its more simple parts. One reactant yields two or more products. Basically, synthesis and decomposition reactions are opposites.
3. *Single replacement reaction*: In a single replacement reaction a single uncombined element replaces another in a compound. Two reactants yield two products.
4. *Double replacement reaction*: In a double replacement reaction parts of two compounds switch places to form two new compounds. Two reactants yield two products.

Chemical changes are a result of chemical reactions. All chemical reactions involve a change in substances and a change in energy. During a chemical reaction, energy is either released (exothermic reactions) or absorbed (endothermic reactions).

3. Numerical solution

3.1. Numerical solution of governing differential equations for water and air flow

The governing differential equations for water flow (1) and air flow (2), as defined in the previous section, have two variables u_w and u_a; these variables are primary unknowns. The primary unknowns can be approximated using the shape function approach as

$$u_w = \hat{u}_w = \sum_1^n N_s u_{ws}; \qquad u_a = \hat{u}_a = \sum_1^n N_s u_{as}$$

where N_s is the shape function, u_{ws} the nodal pore-water pressure, u_{as} the nodal pore-air pressure and n represents the number of nodes in each element. Replacing the primary unknowns with shape functions approximation of above equations, Eqs. (1) and (2) can be written as

$$\nabla(K_{ww}\nabla\hat{u}_w) + \nabla(K_{wa}\nabla\hat{u}_a) + J_w - C_{ww}\frac{\partial\hat{u}_w}{\partial t} - C_{wa}\frac{\partial\hat{u}_a}{\partial t} = R_{\Omega w} \tag{16}$$

$$\nabla(K_{aw}\nabla\hat{u}_w) + \nabla(K_{aa}\nabla\hat{u}_a) + J_a - C_{aw}\frac{\partial\hat{u}_w}{\partial t} - C_{aa}\frac{\partial\hat{u}_a}{\partial t} = R_{\Omega a} \tag{17}$$

where $R_{\Omega w}$ and $R_{\Omega a}$ are the residual errors introduced by the approximation functions. A finite element scheme is applied to the spatial terms employing the weighted residual approach to minimize the residual error represented by Eq. (16) or (17) and integrating the equation over the spatial domain (Ω^e). Spatial discretization of governing differential equation for water flow can be written as

$$C_{ww}\frac{\partial u_{ws}}{\partial t} + C_{wa}\frac{\partial u_{as}}{\partial t} + K_{ww}u_{ws} + K_{wa}u_{wa} = f_w \tag{18}$$

where $C_{ww} = \sum_{e=1}^n \int_{\Omega_e}[N^T C_{ww} N]\,d\Omega_e$; $C_{wa} = \sum_{e=1}^n \int_{\Omega_e}[N^T C_{wa} N]\,d\Omega_e$; $K_{ww} = \sum_{e=1}^n \int_{\Omega_e}[\nabla N^T (K_{ww} N)]\,d\Omega_e$; $K_{wa} = \sum_{e=1}^n \int_{\Omega_e}[\nabla N^T (K_{wa} N)]\,d\Omega_e$; $f_w = \sum_{e=1}^n \int_{\Omega_e}[\nabla N^T (K_w \rho_w \nabla z)]\,d\Omega_e - \sum_{e=1}^n \int_{\Gamma_e} N_r\{\rho_w \hat{v}_{wn} + \rho_w \hat{v}_{vd} + \rho_w \hat{v}_{va}\}\,d\Gamma^e$ in which $\hat{v}_{wn}$ is the approximated water velocity normal to the boundary surface, $\hat{v}_{vd}$ the approximated diffusive vapor velocity normal to the boundary surface, $\hat{v}_{va}$ the approximated pressure vapor velocity normal to the boundary surface and Γ^e is the element boundary surface. Similarly, the spatial discretization

of governing differential equation for air flow leads to:

$$C_{aw}\frac{\partial u_{ws}}{\partial t} + C_{aa}\frac{\partial u_{as}}{\partial t} + K_{aw}u_{ws} + K_{aa}u_{as} = f_a \quad (19)$$

where $C_{aw} = \sum_{e=1}^{n}\int_{\Omega_e}[N^T C_{aw} N]\,d\Omega_e$; $C_{aa} = \sum_{e=1}^{n}\int_{\Omega_e}[N^T C_{aa} N]\,d\Omega_e$; $K_{aw} = \sum_{e=1}^{n}\int_{\Omega_e}[\nabla N^T (K_{aw}\nabla N)]\,d\Omega_e$; $K_{aa} = \sum_{e=1}^{n}\int_{\Omega_e}[\nabla N^T (K_{aa}\nabla N)]\,d\Omega_e$; $f_a = \sum_{e=1}^{n}\int_{\Omega_e}[\nabla N^T (K_w\rho_{da}H_a\nabla z)]\,d\Omega_e - \sum_{e=1}^{n}\int_{\Gamma_e} N^T\rho_{da}\{\hat{v}_{fn} + \hat{v}_{an}\}\,d\Gamma^e$ in which $\hat{v}_{fn}$ is the approximated velocities of free dry air and $\hat{v}_{an}$ is the approximated velocities of dissolved dry air. Spatially discretized equations for coupled flow of water and air, given by the above equations, can be combined in a matrix form as

$$\begin{bmatrix} K_{ww} & K_{wa} \\ K_{aw} & K_{aa} \end{bmatrix}\begin{bmatrix} u_{ws} \\ u_{as} \end{bmatrix} + \begin{bmatrix} C_{ww} & C_{wa} \\ C_{aw} & C_{aa} \end{bmatrix}\begin{bmatrix} \dot{u}_{ws} \\ \dot{u}_{as} \end{bmatrix} - \begin{bmatrix} f_w \\ f_a \end{bmatrix} = 0 \quad (20)$$

where $\dot{u}_{ws} = \partial u_{ws}/\partial t$ and $\dot{u}_{as} = \partial u_{as}/\partial t$.

A time discretization of Eq. (20) is achieved here by application of a fully implicit mid interval backward difference algorithm. Applying a finite difference scheme [35] to Eq. (20) will result in:

$$A^{n+1/2}\phi^{n+1} + B^{n+1/2}\left(\frac{\phi^{n+1} - \phi^n}{\Delta t}\right) + C^{n+1/2} = 0 \quad (21)$$

where

$$A = \begin{bmatrix} K_{ww} & K_{wa} \\ K_{aw} & K_{aa} \end{bmatrix}; \quad B = \begin{bmatrix} C_{ww} & C_{wa} \\ C_{aw} & C_{aa} \end{bmatrix};$$

$$C = \begin{bmatrix} f_w \\ f_a \end{bmatrix}; \quad \phi = \begin{bmatrix} u_{ws} \\ u_{as} \end{bmatrix}$$

Eq. (21) can be further simplified to give:

$$\phi^{n+1} = \left[\frac{A^{n+1/2} + B^{n+1/2}}{\Delta t}\right]^{-1}\left[\frac{B^{n+1/2}\phi^n}{\Delta t - C^{n+1/2}}\right].$$

3.2. Numerical solution of the contaminant transport governing equation

Ignoring the source and sink terms (F^w) Eq. (12) reduces to:

$$\frac{\partial(R\theta c)}{\partial t} + \nabla(vc) - \nabla(D\nabla c) + \lambda c = 0 \quad (22)$$

The primary unknown can be approximated using the shape function approach as

$$\theta c = \theta\hat{c} = \sum_{1}^{n} N_s\theta c_s; \quad c = \hat{c} = \sum_{1}^{n} N_s c_s$$

where c_s is the nodal contaminant concentration and n is the number of nodes per element. In the present work, eight-node quadratic element has been used ($n = 8$). Replacing the primary unknowns with shape function approximation of the above equations employing the Galerkin weighted residual approach to minimize the residual error represented by this approximation the discretized global finite element equation for single component of contaminant takes the form:

$$\frac{M\,dc}{dt} + Hc + F = 0 \quad (23)$$

where $M = \sum_1^n\int_a^b(\theta c/\Delta t)A_{ij}$; $H = \sum_1^n\int_a^b vcB_{ij} + DcE_{ij} + \lambda cA_{ij}$; $F = \sum_1^n N^2(vc - D\partial c/\partial x\partial c/\partial y + \lambda\partial c/\partial x\partial c/\partial y)\big|_a^b$; $A_{ij} = \int NN\,dx\,dy$; $B_{ij} = \int(N\partial N/\partial xN\partial N/\partial y)\,dx\,dy$; $E_{ij} = \int(\partial N/\partial x\partial N/\partial y\partial N/\partial x\partial N/\partial y)\,dx\,dy$.

Applying a finite difference scheme [35] to Eq. (23) will result in:

$$M(\theta c)^{n+1} - \frac{(\theta c)^n}{\Delta t} + H[(1-\gamma)c^n + \gamma c^{n+1}] + F^{n+1} = 0 \quad (24)$$

where Δt is the time step, γ a parameter between 0 and 1 and n and $n+1$ stand for time levels (t_n and $t_{n+1} = t_n + \Delta t$). The solution of Eqs. (21) and (24) will give the distribution of the contaminant concentrations at various points within the soil and at different times, taking into account the interaction between the flow of air and water and various mechanisms of contaminant transport.

4. Numerical results

The developed finite element model is validated by application to two different contaminant transport problems from literature [17,19]. The model is then applied to a case study to predict the transport of contaminant in a site in Australia [33].

4.1. Example 1

In the first example, the developed finite element model is applied to study contaminant transport through a column of saturated sandy soil including the combined effect of advection and dispersion. The soil column has a height of 2 m and a width of 0.02 m as shown in Fig. 2 [17]. The results of the numerical model predictions are compared with those obtained using an analytical solution [3]. The loading system in this analysis

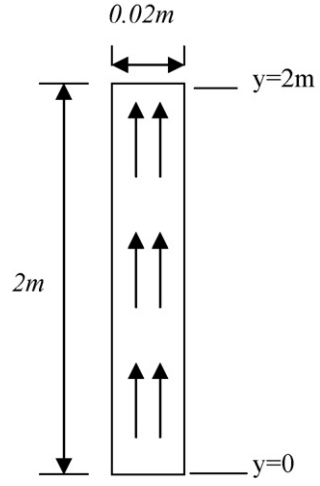

Fig. 2. Problem definition.

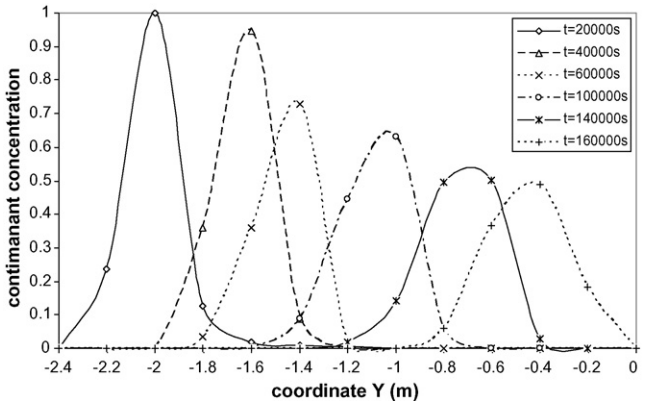

Fig. 3. Variation of concentration distribution with time along the column.

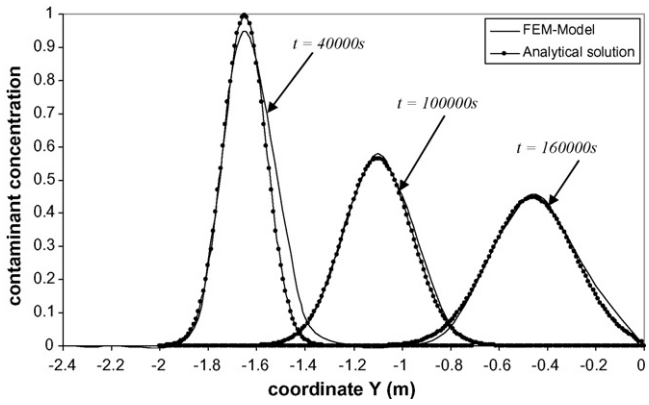

Fig. 4. Comparison of numerical and analytical solutions.

involves the concentration of pollutant, c, picked up by the flow from the base of the column and distributed with time in the vertical direction. The pollutant influx has the form of a pulse entering at the bottom of the soil column and moving upward from the base under the effect of vertical groundwater advective velocity $v_w = 10^{-5}$ m/s. The soil has a porosity of $n = 0.35$. The numerical analysis of the advection and dispersion of the pollutant in the vertical column with $D = 10^{-7}$ m^2/s and a time increment of $\Delta t = 2 \times 10^4$ s is illustrated in Fig. 3 in the form of concentration profiles at different times ($t = 2 \times 10^4$, 4×10^4, 6×10^4 to 1.6×10^5 s). This figure indicates that the pollutant is flowing upwards in the column with the groundwater. The maximum concentration is decreasing gradually from its initial value of the infiltrating mixture ($c_0 = 1$ mol/m^3) due to the effect of advection and dispersion while the width of the pulse increases. The results of the finite element analysis are compared with those of an analytical solution proposed by Appelo and Postma [3] as

$$c = \frac{M}{\sqrt{\pi D t}\exp^{-((y-y_0)^2/4Dt)}} \tag{25}$$

where c is the tracer concentration in (mol/m^3), M in mol/m^2 of cross sectional area normal to the flow, is half of the total mass of the pollutant entering at ($y = 0$) during ($t \geq 0$), D the coefficient of hydrodynamic dispersion in (m^2/s) and y_0 is the location of the maximum concentration which is ($y_0 = 0$) at ($t = 2 \times 10^4$) [17]. The numerical and analytical solutions are shown for three times steps of ($t = 4 \times 10^4$, 1×10^5 and 1.6×10^5 s) in Fig. 4. Comparison of the results shows a very good agreement between the results of the numerical model and the analytical solution.

4.2. Example 2

To illustrate the capabilities of the model to predict the effects of other mechanisms of contaminant transport, another example involving the combined effect of advection, diffusion–dispersion and adsorption is considered. In this example a one-dimensional transport of a contaminant through a bar, 30 m long and 1 m high, is considered. The bar is subjected to an initial Gaussian contaminant distribution of amplitude $c = 1$ centered at $x = 5.0$ m (see

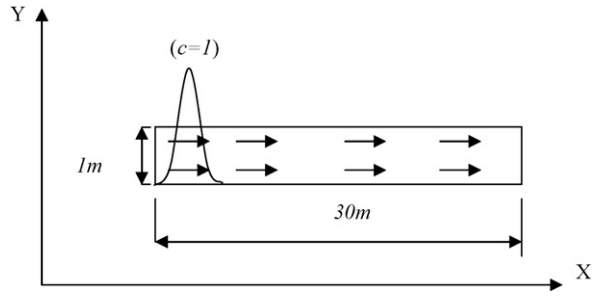

Fig. 5. Problem definition.

Fig. 5) and the boundary conditions are $c = 0$ on the left and right boundaries and zero flux on the top and bottom boundaries. A steady and uniform intrinsic velocity field with $v_w = 1$ m/s is assumed over the bar. In the first case, only the transport of the contaminant by advection is considered. Fig. 6 shows the distribution of contaminant concentration along the bar at times $t = 0$, 10 and 20 s. It is shown that the results of the developed model are in close agreement with those reported by Li et al. [19] for this example. To illustrate the capabilities of the model to predict the effects of other mechanisms of contaminant transport, another case involving the combined effect of advection and diffusion–dispersion is considered and the result are shown in Fig. 7. In this case, the same initial Gaussian distribution of concentration, as in the previous case, is considered together with

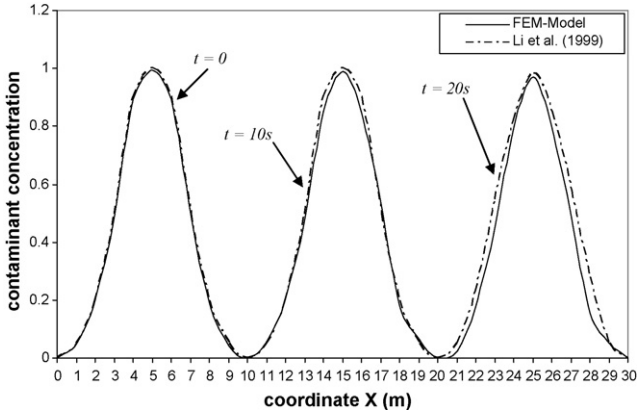

Fig. 6. Concentration distributions at $t = 0$, 10 and 20 s.

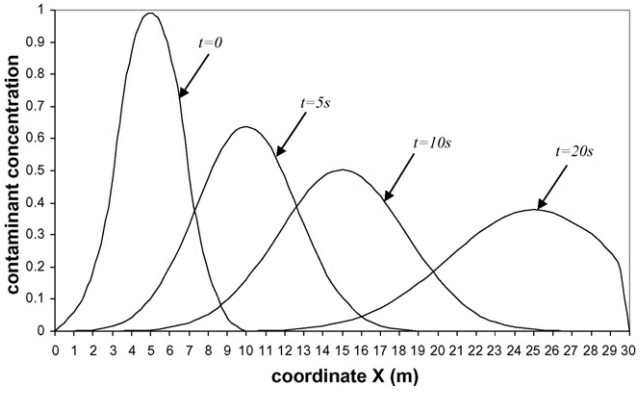

Fig. 7. Contaminant concentration distributions at (t = 0, 5, 10 and 20 s) for advection and diffusion–dispersion.

additional diffusion and dispersion parameters including the longitudinal dispersivity for water phase $\alpha_{L_W} = 0.5$, the coefficient of water molecular diffusion $D_{m_w} = 0$ and the reaction rate for water phase $\lambda_w = 0$. Fig. 7 shows the distribution of contaminant concentration a long the bar due to the combined effect of advection and dispersion at times t = 0, 5, 10 and 20 s. It is seen that the distribution of the contaminant concentration continuously decreased from the initial amplitude of $c = 1$ due to the effect of the dispersion mechanism. Fig. 8 shows the distribution of contaminant concentration along the bar due to the combined effect of advection and dispersion at time t = 10 s. Again, it is shown that the results of the model are in very good agreement with those reported by Li et al. [19] for this case. To investigate the effect of adsorption, a third case involving the combined effect of advection, dispersion, diffusion and adsorption is considered. The result for this case is shown in Fig. 9. Again, the same initial Gaussian distribution of concentration, as in the previous cases, is considered together with additional adsorption parameters including volumetric content of the solid $\theta_s = 2.7$ and distribution coefficient $K_d = 0.01$. Fig. 9 shows the distribution of contaminant concentration along the bar for two cases of with and without consideration of adsorption. It is shown that, as expected, adsorption has caused additional decrease in concentration.

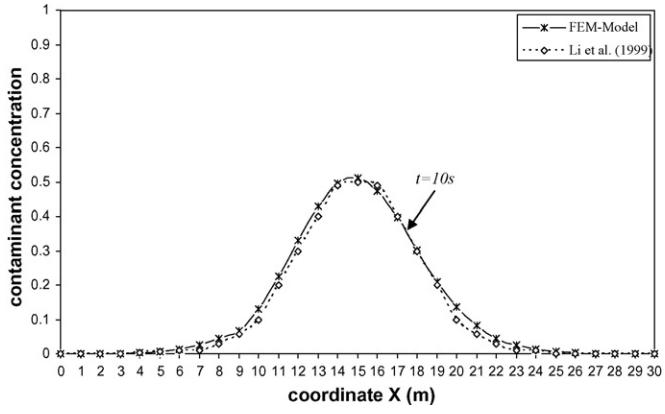

Fig. 8. Concentration distributions at t = 10 s for advection and diffusion–dispersion.

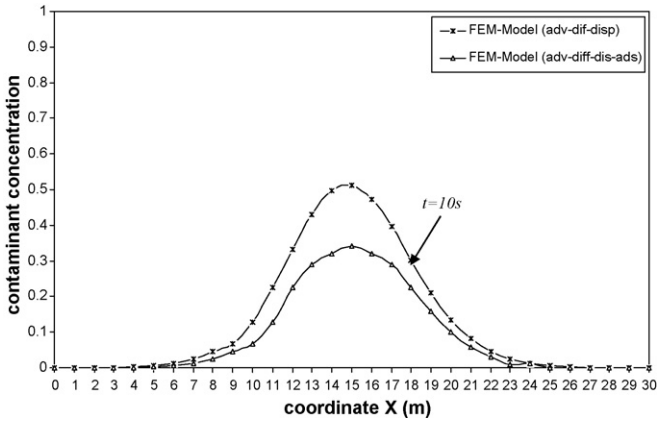

Fig. 9. Concentration distributions at t = 10 s for two cases of with and without adsorption.

4.3. Case study

The developed finite element model is also applied to a case study. The case study involves a physical test, conducted by Stagnitti et al. [34], to study the combined effect of advection, diffusion–dispersion, adsorption and chemical reactions on contaminant transport. In this experiment a large, undisturbed soil core (42.5 cm × 42.5 cm on plan and 40 cm deep) (see Fig. 10) was extracted from a farm located about 300 km west of Melbourne in Australia. The farm was used primarily for beef cattle grazing, and superphosphate had not been applied for approximately 25 years [34]. In the experiment, a multiple sample percolation system (MSPS) was used to sample moisture and chemicals leaching from the soil core. The system consisted of a metal-alloy base-plate that was shaped into 25 equal sized collection wells (funnels). The soil core was irrigated by a purpose-built drip irrigation system.

The area coverage, speed, and direction of irrigation were adjustable and were controlled such that the irrigation system could deliver a constant and uniform application of water and soluble nutrients on the soil surface. The soil core was irrigated with distilled water for several months prior to the application of the nutrient solution. An irrigation rate of 2.82 ml/min, comparable with the mean daily rainfall for the region, was uniformly applied to the surface of the soil core. A solution containing 0.1 mol of NaCl, 0.01 mol of KNO_3 and 0.1 mol of KH_2PO_4 was prepared. A total of 1967 ml of this solution was irrigated on the soil surface. Following application of this solution, distilled water was irrigated on the soil surface at the same rate for 18 days. Leachate solutions were analyzed for chloride (Cl), nitrate (NO_3^-), and phosphate (PO_4^{3-}). The daily leachate concentrations collected from each of the 25 individual collection wells were aggregated to calculate a total daily concentration for the entire soil core for each ion for each day of the duration of the experiment. Samples were collected every 12 h from wells that drained more than 50 ml. Wells that had less than 50 ml were left until at least the next collection period, 12 h later.

The developed finite element model was used to simulate the percolation of the solution through the soil block in the experiment. The results of the analysis are shown in Figs. 11–13

(a)

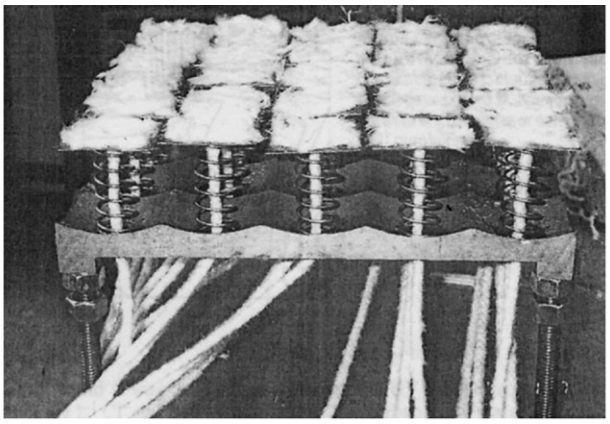

(b)

21	22	23	24	25
16	17	18	19	20
11	12	13	14	15
6	7	8	9	10
1	2	3	4	5

(c)

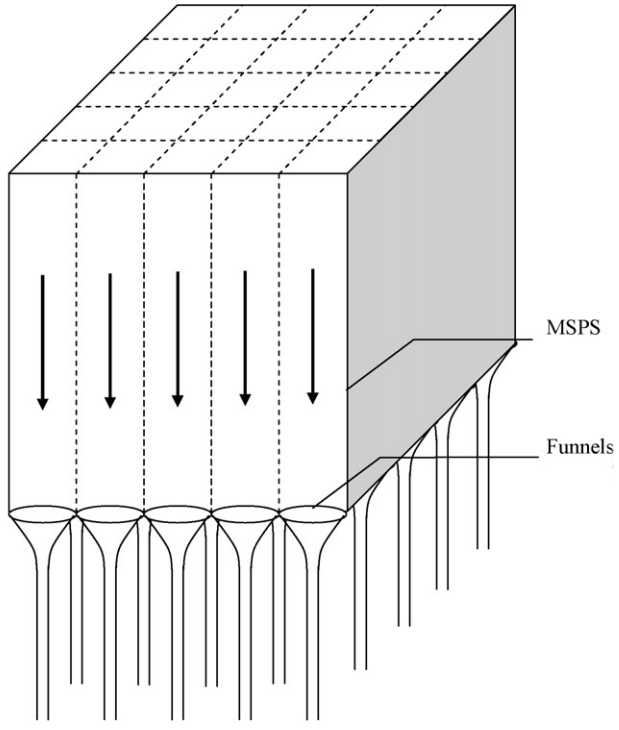

Fig. 10. (a) View of the multiple sample percolation system (MSPS) [34]. (b) Location of collection wells in the MSPS [34]. (c) Problem definition.

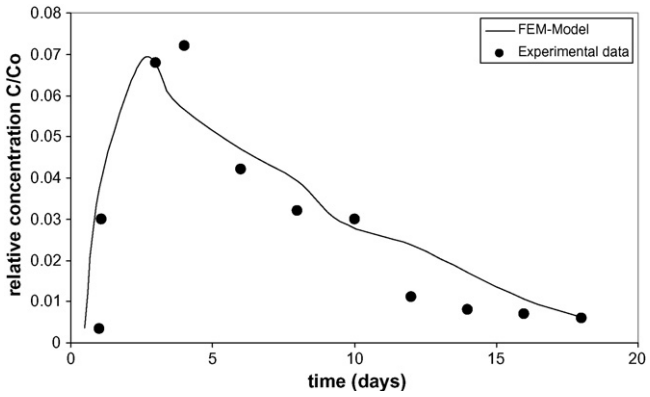

Fig. 11. Breakthrough curves for chloride (Cl).

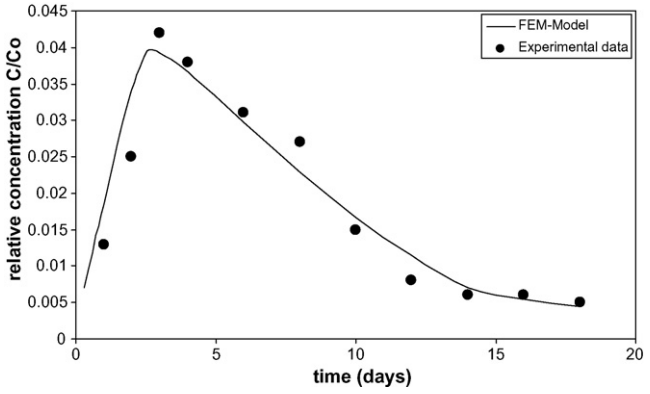

Fig. 12. Breakthrough curves for nitrate (NO_3^-).

in the form of variations of concentrations of chloride, nitrate and phosphate in the soil with time. The figures include the experimental data from the tests conducted by Stagnitti et al. [33]. The initial solute concentrations (c_0) in the irrigation were c_0–Cl = 6186.10 mg/l, c_0–NO_3 = 273.65 mg/l, and c_0–PO_4 = 4724.10 mg/l [33]. Using these values and assuming that C1 behaves as a conservative component, a chemical reaction coefficient of $\lambda = 0$ (no reaction) and a retardation factor of $R = 1$ (no adsorption) were used in the finite element model.

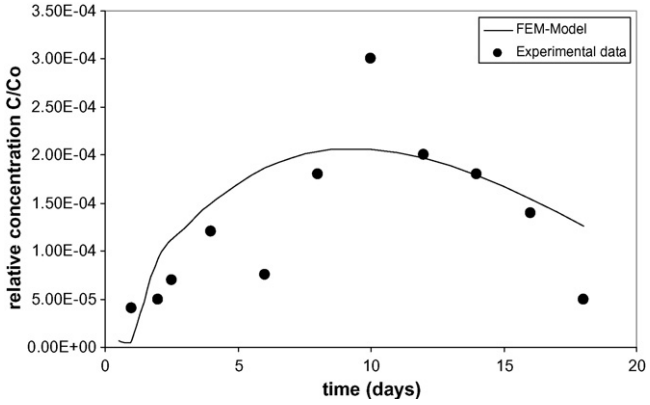

Fig. 13. Breakthrough curves for phosphate (PO_4^{3-}).

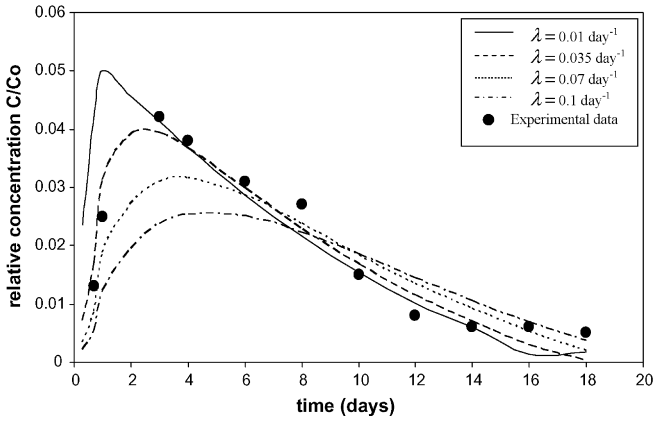

Fig. 14. Variation of relative concentration with time for different rates of reaction for nitrate (NO_3^-).

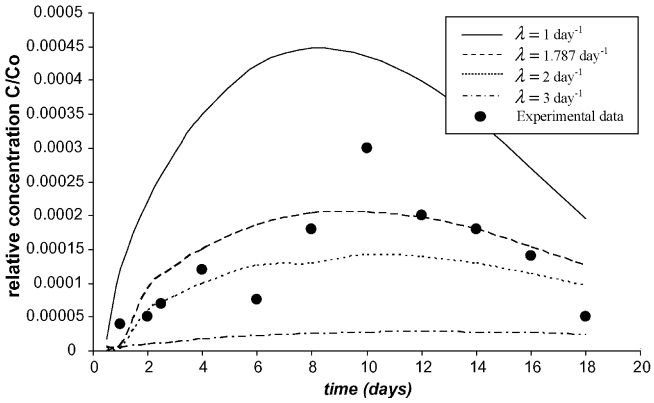

Fig. 15. Variation of relative concentration with time for different rates of reaction for phosphate (PO_4^{3-}).

Also, a water velocity of $v_w = 0.051$ m/day and dispersion coefficient of the pollutant in the vertical column $D = 0.006$ m^2/day were used [33]. Fig. 11 shows the solute breakthrough curve for chloride (Cl) at the bottom of the multiple sample percolation system (MSPS). It is shown that the results of the developed numerical model are in close agreement with the experimental results reported by Stagnitti et al. [33]. The predicted breakthrough curve (BTC) for nitrate (NO_3^-) using the finite element model is plotted in Fig. 12 together with the experimental data. In this case, the adsorption and reaction of NO_3^- are possible and therefore, R and λ take non-zero values. Values of $R = 1.06$ and $\lambda = 0.035$ day^{-1} are used in the finite element model, indicating a small adsorption and significant reaction rate, as indicated by Stagnitti et al. [33]. The results of the numerical model presented in this paper are in close agreement with the experimental results. Fig. 13 shows the breakthrough curve predicted using the numerical model for (PO_4^{3-}) together with the experimental results. The values of $R = 8.117$ and $\lambda = 1.781$ are used in the model. These values, which were suggested by Stagnitti et al. [33], indicate very strong adsorption and quick reaction. The results show that the numerical model predicted the changes in concentration of PO_4^{3-} with time reasonably well considering the scatter in the experimental data. In this experiment, three different chemicals with different degrees of retardation and reaction were considered and the model predictions are in close agreement with the experimental results. This illustrates the robustness of the developed finite element model in simulating the effects of chemical reactions on contaminant transport process.

4.3.1. Sensitivity analysis

Sensitivity is a measure of the effect of change in one factor on another factor. The sensitivity of a model dependent variable to a model input parameter is the partial derivative of the dependent variable with respect to that parameter [21,22]. Figs. 14 and 15 show the effect of the chemical reaction coefficient (λ) on concentration breakthrough curves for nitrate (NO_3^-) and phosphate (PO_4^{3-}) respectively, at an observation point. It can be seen that chemical reactions play a significant role in transport and changes in concentrations of NO_3^- and PO_4^{3-} with time. In both cases, the peak of the concentration curves rises with decreasing the value of the chemical reaction coefficient (λ). This analysis indicates the importance of consideration of the effect chemical reactions in modeling the transport of reactive contaminants in soils.

5. Conclusions

One of the most challenging problems in modeling of solute transport in soils is how to effectively characterize and quantify the effects of chemical reactions on the transport process. Recent studies have shown that the current models of contaminant transport analysis are not able to adequately describe the effects of chemical reactions. Furthermore, the effect of chemical reactions on the fate and transport of contaminants is not included in many of the existing numerical models for contaminant transport. This paper presented a coupled transient finite element model for predicting the flow of air and water and contaminant transport in unsaturated soils including the effect of chemical reactions. The model is capable of simulating various phenomena governing miscible contaminant transport in soils including advection, dispersion, diffusion, adsorption and chemical reaction effects. The mathematical framework and the numerical implementation of the model were presented. The model was validated by application to two test cases from the literature and was then applied to simulation of a physical model test involving transport of contaminants in a block of soil with the aim of studying the effects of chemical reactions on contaminant concentration and transport. In the experiments, three different chemicals with different degrees of retardation and reaction were considered. The numerical results illustrated the performance of the presented model in simulating the effects of different phenomena governing the transport of contaminants in soils. The finite element model performed well in predicting transport of contaminants through the soil with and without inclusion of the effects of chemical reactions. Comparison of the results of the numerical model with the experimental results shows that the model is capable of predicting the effects of chemical reactions with very high accuracy. The sensitivity analysis highlighted the importance of consideration of chemical reactions in modeling of contaminant transport in soils and showed that chemical

reactions can have a significant effect on the concentration of contaminants in soils.

References

[1] L. Abriola, G.F. Pinder, A multiphase approach to the modeling of porous media contaminated by organic compounds. 1. Equation development, Water Resour. Res. 21 (1985) 11–18.

[2] L.R. Ahuja, O.R. Lehman, The extent and nature of rainfall–soil interaction in the release of soluble chemicals to runoff, J. Environ. Qual. 12 (1983) 34–40.

[3] C.A.J. Appelo, D. Postma, Geochemistry Groundeater and Pollution, A.A. Balkema, Rotterdam, Netherlands, 1993.

[4] C. Arsene, Migration behaviour of ^{3}H ^{14}C and ^{241}AM in unsaturated soils, in: Proceeding of the International Conference Nuclear Energy in Central Europe, Bled, Slovenia, 2000.

[5] J. Bear, Dynamics of Fluids in Porous Media, American Elsevier Publishing Company, Inc., Amsterdam, The Netherlands, 1979.

[6] M.A. Celia, E.T. Boluloutas, A general mass-conservative numerical solution for the unsaturated flow equation, Water Resour. Res. 26 (7) (1990) 1483–1496.

[7] J.A. Cherry, R.W. Gillham, J.F. Barker, Contaminant in groundwater: chemical processes, in: Groundwater Contamination, National Academy Press, Washington, DC, USA, 1984, pp. 46–64.

[8] T.P. Clement, B.S. Hooker, R.S. Skeen, Numerical modeling of biologically reactive transport near nutrient injection well, J. Environ. Eng. 122 (9) (1996) 833–839.

[9] N. Depountis, Geotechnical Centrifuge Modeling of Capillary Phenomena and Contaminant Migration in Unsaturated Soils. PhD Dissertation, University of Cardiff, UK, 2000.

[10] P. Engesgaard, K.L. Kip, A geochemical model for redox-controlled movement of mineral fronts in ground-water flow systems: a case of nitrate removal by oxidation of pyrite, Water Resour. Res. 28 (10) (1992) 2829–2843.

[11] H. Gao, V. Vesovic, A. Butler, H. Wheater, Chemically reactive multicomponent transport simulation in soil and groundwater: 2. Model demonstration, Environ. Geol. 41 (2001) 280–284.

[12] R.W. Gillham, J.A. Cherry, Contaminant migration in saturated unconsolidated geologic deposits, Geol. Soc. Am. Special Paper 189 (1982) 31–61.

[13] E.E. Hellawell, C. Sawidou, A study of contaminant transport involving density driven flow and hydrodynamic clean up, in: Proceedings of the Centrifuge '94 Conference, University of Cambridge, UK, 1994.

[14] A.A. Javadi, M.M. AL-Najjar, A.S.I. Elkassas, Finite element modeling of contaminant transport in soil, in: Proceeding of the International Conference on Problematic Soils, Eastern Mediterranean University, Cyprus, 2005, pp. 283–290.

[15] A.A. Javadi, M.M. AL-Najjar, A.S.I. Elkassas, Numerical modeling of contaminant transport in unsaturated soil, in: Proceeding of the 5th International Congress on Environmental Geotechnics, Cardiff, UK, 2006, pp. 1177–1184.

[16] J. Kacur, B. Malengier, M. Remesikova, Solution of contaminant transport with equilibrium and non-equilibrium adsorption, J. Comput. Methods Appl. Mech. Eng. 194 (2005) 479–489.

[17] H.M. Karkuri, F. Molenkamp, Analysis of advection dispersion of pollutant transport through a layered porous media, in: Proceeding of the International Conference on Geoenvironmental Engineering, Cardiff, UK, 1997, pp. 193–198.

[18] J.S. Kindred, M.A. Celia, Contaminant transport and biodegradation. 2. Conceptual model and test simulations, Water Resour. Res. 25 (6) (1989) 1149–1159.

[19] X. Li, S. Cescotto, H.R. Thomas, Finite element method for contaminant transport in unsaturated soils, J. Hydrol. Eng. 4 (3) (1999) 265–274.

[20] I.S. Metcalfe, Chemical Reaction Engineering, Oxford University Press, Oxford, UK, 1997.

[21] C.D. McElwee, Sensitivity analysis and the ground water inverse problem, Ground Water 20 (6) (1982) 723–735.

[22] C.D. McElwee, Sensitivity analysis of ground water models, in: Advanced in Transport Phenomena in Porous Media, NATO Advanced Study Institute Series, 1987, pp. 751–817.

[23] B.P. McGrail, Inverse reactive transport simulator (INVERTS): an inverse model for contaminant transport with nonlinear adsorption and source terms, Environ. Model. Software 16 (2001) 711–723.

[24] E.V. Mironenko, Y.A. Pachepsky, Estimating transport of chemicals from soil to ponding water, J. Hydrol. 208 (1998) 53–61.

[25] W.W. Nazaroff, L. Alvarez-Cohen, Environmental Engineering Science, John Wiley & Sons, Inc., USA, 2001.

[26] K.J. Osinubi, C.M.O. Nwaiwu, Sodium diffusion in compacted lateritic soil, in: Proceeding of the 5th International Congress on Environmental Geotechnics, Cardiff University, UK, 2006, pp. 1224–1231.

[27] D.L. Parkhurst, D.C. Thorstenson, L.N. Plummer, PHREEQC—A Computer Program for Geochemical Calculations. US Geological Survey Techniques of Water Resources Investigations Report, 1980, pp. 99–4259.

[28] J. Rubin, Transport of reacting solutes in porous media; relation between mathematical nature of problem formulation and chemical nature of reactions, Water Resour. Res. 35 (8) (1983) 2359–2373.

[29] J. Rubin, R.V. James, Dispersion affected transport of reacting solutes in saturated porous media—Galerkin method applied to equilibrium controlled exchange in unidirectional steady water flow, Water Resour. Res. 9 (5) (1973) 1332–1356.

[30] H.S. Sethi, A 3-Dimensional Finite Element Method for Groundwater Flow and Contaminant Transport. PhD Dissertation, Department of Mechanical Engineering, University of Nevada, Las Vegas, USA, 1995.

[31] D. Sheng, D.W. Smith, 2D finite element analysis of multicomponent contaminant transport through soils, Int. J. Geomech. 2 (1) (2002) 113–134.

[32] I.K. Snyder, D.A. Woolhiser, Effect of infiltration on chemical transport into overland flow, Trans. Am. Soc. Agric. Eng. 28 (1985) 1450–1457.

[33] F. Stagnitti, L. Li, A. Barry, G. Allinson, J.Y. Parlange, T. Steenhuis, E. Lakshmanan, Modeling solute transport in structured soils: performance evaluation of the ADR and TRM models, Math. Comput. Model. J. 34 (2001) 433–440.

[34] F. Stagnitti, J. Sherwood, G. Allinson, L. Evans, M. Allinson, L. Li, I. Phillips, An investigation of localised soil heterogeneities on solute transport using a multisegment percolation system, NZ J. Agric. Res. 41 (1998) 603–612.

[35] L.F. Stasa, Applied Finite Element Analysis for Engineers, Holt, Rinehart and Winston Inc., USA, 1985.

[36] D. Stoicheva, M. Kercheva, V. Koleva, Assessment of nitrate leaching under different nitrogen supply of irrigated maize, in: A. Bieganowski, G. Jozefaciuk, R. Walczak (Eds.), Modern Physical and Physicochemical Methods and their Application in Agroecological Research, Institute of Agrophysics, PAS, Lublin, 2004, pp. 208–218.

[37] D. Stoicheva, M. Kercheva, D. Stoichev, NLEAP water quality applications in Bulgaria, in: M. Shaffer, L. Ma, S. Hansen (Eds.), Modeling Carbon and Nitrogen Dynamics for Soil Management, Lewis Publishers, Boca Raton, FL, 2001, pp. 333–345.

[38] D. Stoicheva, M. Kercheva, D. Stoichev, Nitrogen distribution in vadose zone under some Bulgarian soils, in: Proceeding of the 5th International Congress on Environmental Geotechnics, Cardiff University, UK, 2006, pp. 1256–1263.

[39] H.R. Thomas, Y. He, A coupled heat–moisture transfer theory for deformable unsaturated soil and its algorithmic implementation, Int. J. Numer. Methods Eng. 40 (1997) 3421–3441.

[40] R. Wallach, G. Grigorin, J. Rivlin, A comprehensive mathematical model for transport of soil-dissolved chemicals by overland flow, J. Hydrol. 247 (2001) 85–99.

[41] A.L. Walter, E.O. Frind, D.W. Blowes, C.J. Ptacek, J.W. Molson, Modelling of multicomponent reactive transport in groundwater. 1. Model development and evaluation, Water Resour. Res. 30 (1994) 3137–3148.

[42] J.M. Yan, K. Vairavmoorthy, 2D numerical simulation of water flow and contaminant transport in unsaturated soil, in: Proceeding of the 6th International Conference on Hydroinformatics, 2004, pp. 1–8.

[43] G.T. Yeh, V.S. Tripathi, A critical evaluation of recent development of hydro-geochemical transport model of reactive multi-chemical components, Water Resour. Res. 25 (1) (1989) 93–108.
[44] R.N. Yong, A.M.O. Mohamed, B.P. Warkentin, Principles of Contaminant Transport in Soils, Elsevier Science, Amsterdam, The Netherlands, 1992.
[45] Z. Zhang, M.L. Brusseau, Nonideal transport of reactive contaminants in heterogeneous porous media: 7. Distributed-domain model incorporating immiscible-liquid dissolution and rate-limited sorption/desorption, J. Contamin. Hydrol. 74 (2004) 83–103.
[46] C. Zheng, G.D. Bennett, Applied Contaminant Transport Modeling, Papadopulos & Associates Inc., Bethesda, Maryland, 2002.